*Carbohydrate Polymers* **8** (1988) 45–53

# A Study of Amylose Gelation Using a Synchrotron X-Ray Source

K. J. I'Anson, M. J. Miles, V. J. Morris, S. G. Ring

AFRC Institute of Food Research, Norwich Laboratory, Colney Lane, Norwich NR4 7UA, UK

and

C. Nave

SERC Daresbury Laboratory, Warrington WA4 4AD, UK

(Received 18 February 1987; revised version received 29 April 1987; accepted 3 August 1987)

*SUMMARY*

*Time-dependent studies of the gelation of amylose have been made using the Daresbury Synchrotron X-ray source. Both small-angle scattering (SAXS) and wide-angle diffraction (WAXD) studies were made during gelation. These data were supplemented with SAXS and WAXD data obtained using a conventional X-ray source and measured as a function of time of storage of the gels. These data have been used to assess the role of crystallinity in the gelation process.*

## INTRODUCTION

Amylose is defined as the linear polysaccharide, composed of $\alpha(1\rightarrow4)$ linked D-glucose, which is solubilized from swollen gelatinized starch granules. Amylose solutions of sufficiently high concentration gel upon cooling to room temperature. Gelation of amylose plays an important role in the gelation of starch (Miles *et al.*, 1985*a*), but it is also of wider interest to the general study of polymer gelation. This note reports the use of a synchrotron X-ray source to probe the time-dependent changes in molecular association during gelation in order to investigate mechanisms of gelation.



*Carbohydrate Polymers* 0144-8617/88/$03.50 — © 1988 Elsevier Applied Science Publishers Ltd, England. Printed in Great Britain

The primary mechanism for amylose gelation has been attributed to phase-separation (Miles *et al.*, 1984, 1985*b*). This suggestion arose from the observation that phase separation, as monitored by the accompanying volume change and the development of turbidity, occurred on a similar time-scale to the development of the polymer network, as monitored by measurements of shear modulus. The actual rates were found to depend upon experimental conditions such as polymer concentration and quench temperature or quenching rate.

For example, a 2·4% solution of pea amylose quenched to 32°C showed an initial rapid increase in turbidity, volume change, and shear modulus which occurred within the first 100 min. For a 7% solution the time-scale was reduced to about 10 min. Crystallization, as monitored by the appearance of the 100 diffraction maximum characteristic of the B-type crystalline form of amylose, was found to occur over a longer time-scale and the rate of crystallization was found to be independent of the total amylose concentration in the concentration region 2·4–7%. Based on these observations it was suggested (Miles *et al.*, 1984, 1985*b*) that crystallization was not the primary mechanism of gelation but occurred within the polymer-rich phase subsequent to the phase separation. Thermodynamic considerations require that if crystallization does occur within a system quenched into the biphasic region then it must occur subsequently to the phase separation.

A phase-separated, polymer-rich, network may in itself be sufficient to produce gel-like behaviour, the restoring force being attributed to the surface energy associated with the large interfacial surface area of the phases and the visco-elastic nature of the molecular entanglements within the polymer-rich phase. An alternative mechanism would involve the formation of a phase-separated, polymer-rich network structure which is subsequently stabilized and consolidated by amylose crystallization or vitrification. This note reports small-angle scattering (SAXS) and wide-angle diffraction (WAXD) X-ray studies carried out during gelation in order to assess the role played by crystallization.

Studies were made on the gelation of a 6% amylose solution following quenching from 75 to 22°C. The source and preparation of the amylose is as reported in previous studies (Miles *et al.*, 1984, 1985*a*, *b*). Conventional X-ray sources have been employed to follow phase separation in synthetic polymer systems (Khambatta *et al.*, 1976; Hashimoto *et al.*, 1986). Synchrotron X-ray radiation was used in the studies reported here because its high intensity is essential in order to enable sufficiently rapid data collection during the early stages of gelation. SAXS data were initially recorded photographically. Later experiments made use of a linear, position-sensitive detector and data were recorded in time slots of

2 min. A plot of scattered intensity against scattering angle for a series of time slices is shown in Fig. 1. Changes in both intensity and slope at small angles with time can be discerned (Fig. 1). The value of scattered intensity at zero angle, $I(0)$, was extrapolated from $I$ vs $q^2$ plots. Figure 2 shows $I(0)$ plotted against time. An initial rapid increase in $I(0)$ coincident with the increase in shear modulus was observed in about the first 15 min. This was followed by a slower increase in $I(0)$ over longer times during which the shear modulus remained essentially constant. Changes in $I(0)$ may arise from electron-density differences resulting from either phase separation or crystallization. WAXD measurement over the same period of time revealed no discernible diffraction peaks. However, this cannot exclude the presence of a low concentration of small and/or imperfect crystallites. In order to assess the contribution to $I(0)$ from crystallization $I(0)$ was measured over a longer time scale covering the period in which the 100 diffraction maximum, which has an interplanar spacing of 1·58 nm, could be detected. These additional measurements of $I(0)$, and of the diffraction peak, were made using a conventional

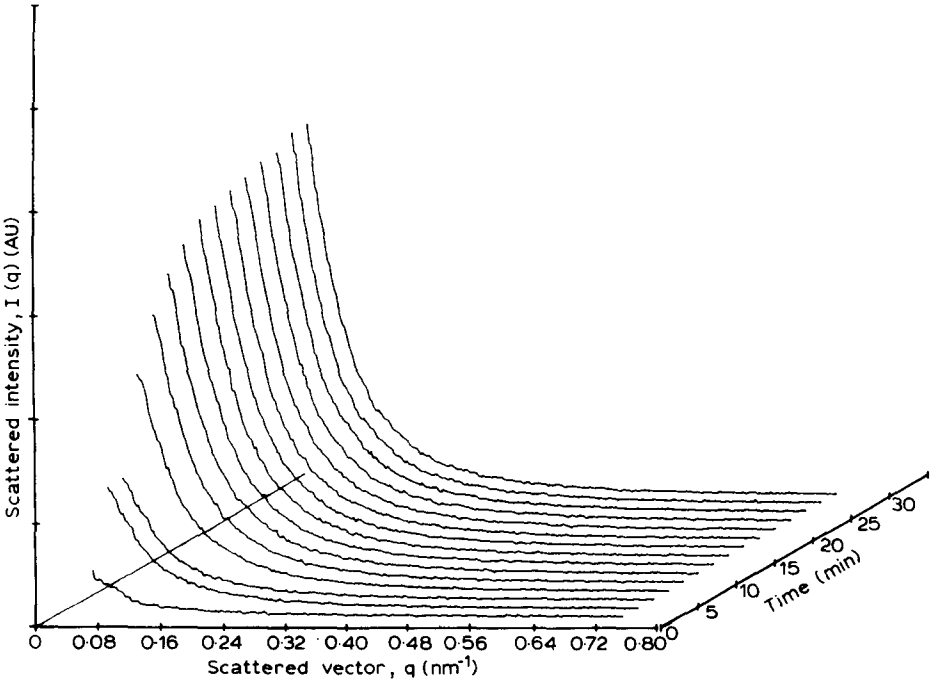


**Fig. 1.** Time-dependent changes in the small-angle X-ray scattering from a 6% amylose solution after quenching from 75 to 22°C. The scattering intensity has been corrected for detector response and normalized to a constant beam current.

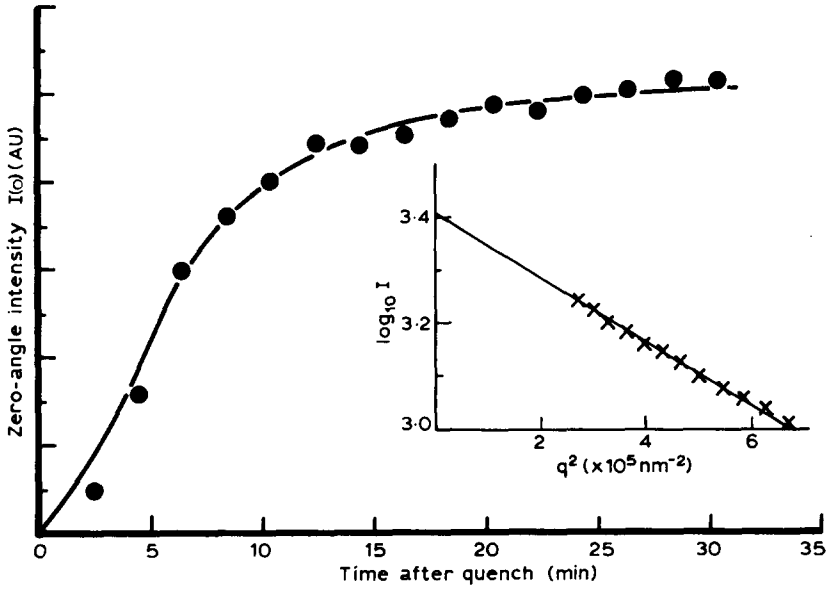


**Fig. 2.** Plot of the scattering intensity extrapolated to zero angle $I(0)$ as a function of elapsed time after quenching. Inset is a typical Guinier plot used in this extrapolation.

X-ray generator and a Kratky camera because the changes occurred more slowly at these longer times after quenching.

Figure 3a and b show respectively the change in $I(0)$ with time and the change in the 100 diffraction-peak area with time. If the electron-density difference of the scatterers is constant, the scattered intensity at zero angle, $I(0)$, depends on the volume of each scattering region and the number of regions. If it is assumed that the size distribution of the scatterers remains constant with time, then $I(0)$ is proportional to the number and therefore the total volume of the regions contributing to the scattering. Figure 4 shows that the size of the scattering regions as determined by the initial slope of the Guinier plots (log $I$-vs-$q^2$), became approximately constant after 5 min, indicating that the above assumption is valid for this system after this time. Further support for constant size distribution is found in the near constant values of correlation length of 8·85 nm after 9 min and 8·26 nm after 29 min determined from the Debye–Bueche plots (Debye & Bueche, 1949; Khambatta *et al.*, 1976) shown in Fig. 5. The area under the $d_{100}$ diffraction peak will depend on the total mass of crystallites present in the gel. The fact that the plots of $I(0)$ and $d_{100}$ peak area against time are, within experimental accuracy, the same suggests that the two parameters are following the same change, namely, crystallization.

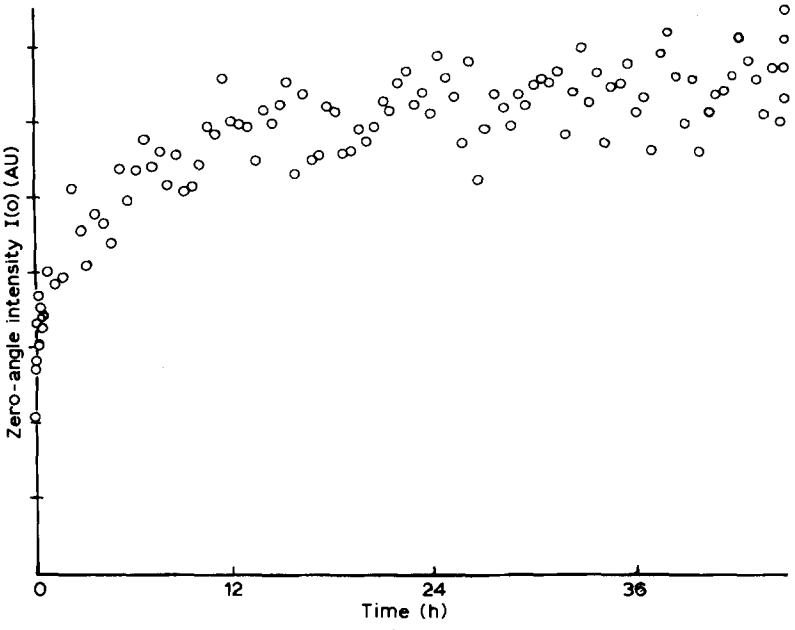


(a)

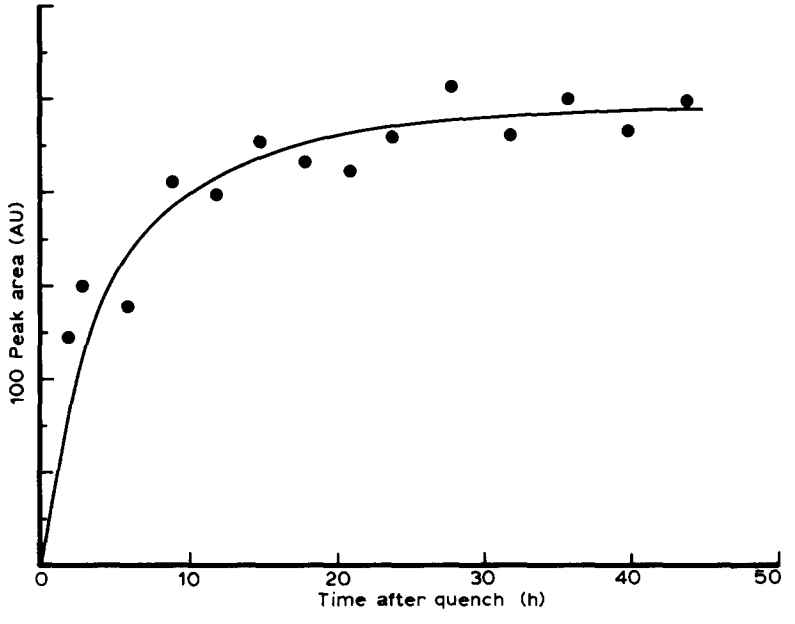


(b)

**Fig. 3.** (a) Plot of the scattering intensity extrapolated to zero angle $I(0)$ as a function of time as measured using the Kratky camera. (b) Plot of the area under the 100 diffraction peak as a function of time measured using the Kratky camera to scan through the appropriate angular range.

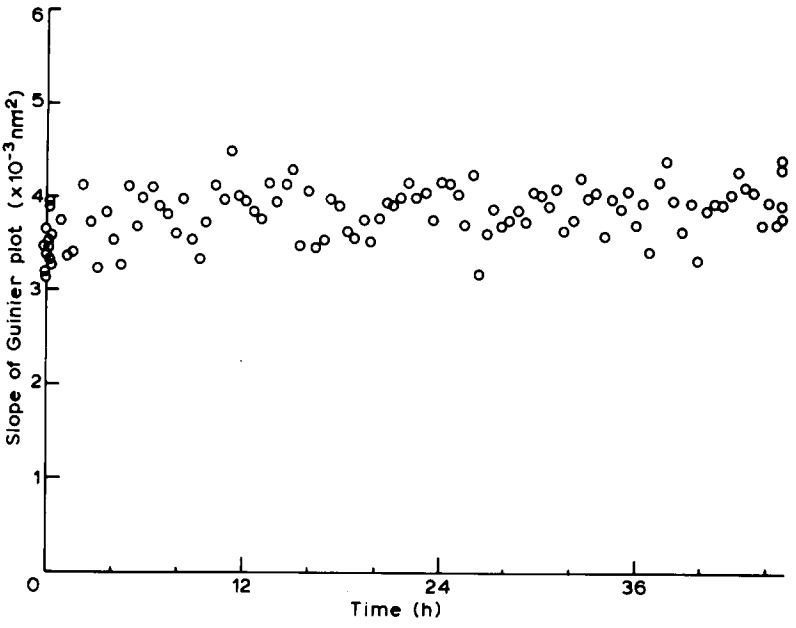


**Fig. 4.** Plot of slope of Guinier plots against time from quench.

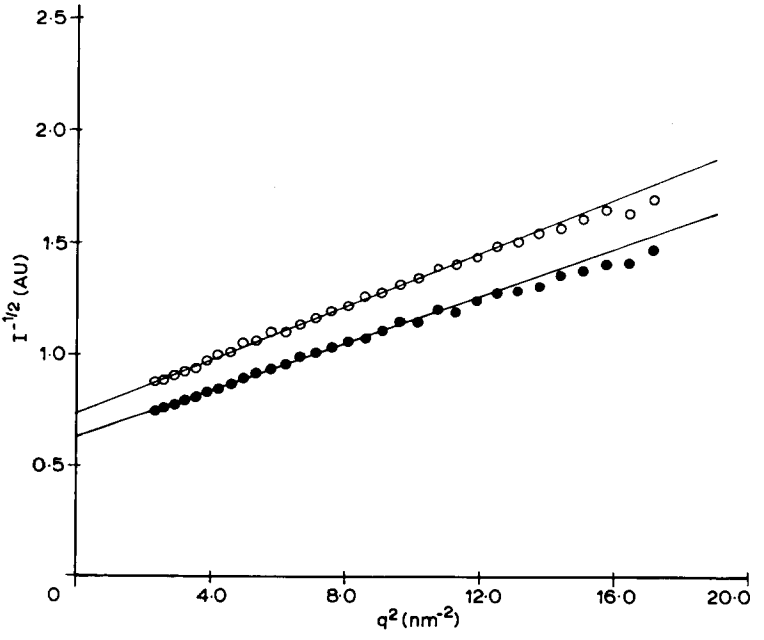


**Fig. 5.** Debye–Bueche plots, $I(q)^{-1/2}$ vs. $q^2$ where $I(q)$ is the scattered intensity at scattering vector, $q$, for data collected after 9 min (○) and after 29 min (●). The correlation length, $lc$ (given by slope/intercept), has values of 8·85 and 8·26 nm, respectively.

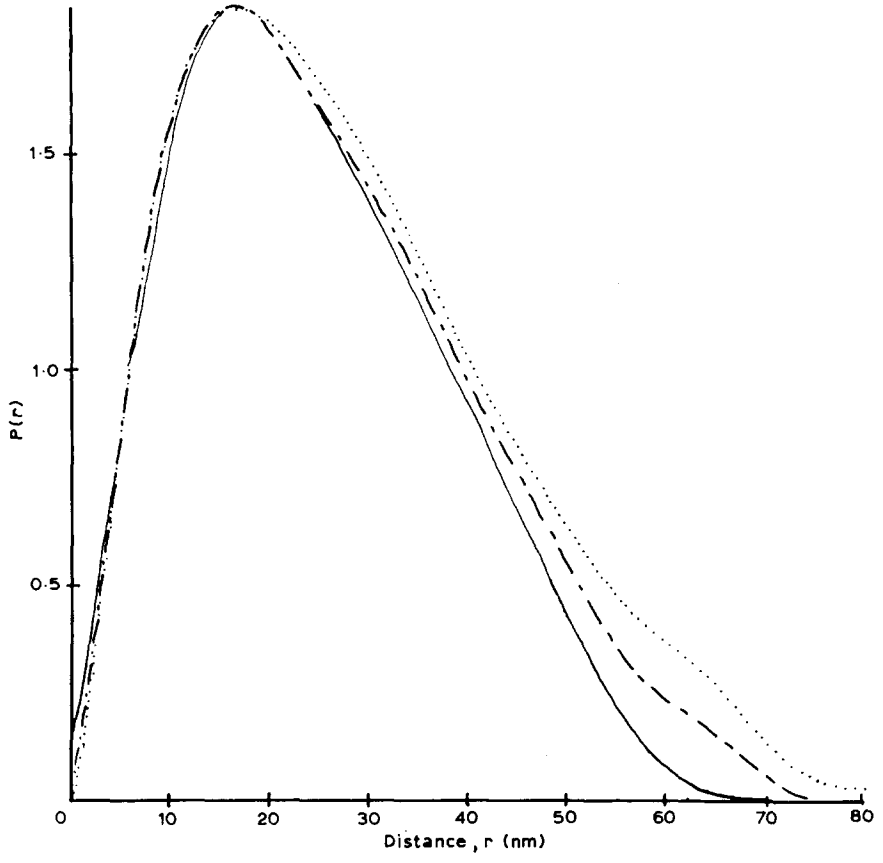


**Fig. 6.** Distance–distribution, $P(r)$, plots from scattering data collected after 4 min (– – –), 9 min (-·-) and 29 min (····).

Distance–distribution function, $P(r)$ (Glatter, 1982) calculated from the scattering data measured after 4, 9 and 29 min are shown in Fig. 6. The shape of these distributions resembles that expected for rod-like scatterers (Glatter, 1982). From these plots, the maximum distance of 70 nm would correspond to the length of the rod. The radius of gyration of such a rod is $70/\sqrt{12}$ nm, i.e. 20·2 nm. This value is in agreement with the value of 20·4 nm determined from the Guinier plot and the $P(r)$ function (Fig. 6) of 22·4 nm. These results suggest an extended-chain morphology for the crystallization of amylose in the gel.

At times less than about 2 h, the $d_{100}$ diffraction signal was too weak to be clearly identified above the background noise, and so the correlation between peak area and $I(0)$ could not be continued to shorter times. However, changes in $I(0)$ were detected from the first 2 min following quenching. Figure 7 shows that the changes in $I(0)$ associated with

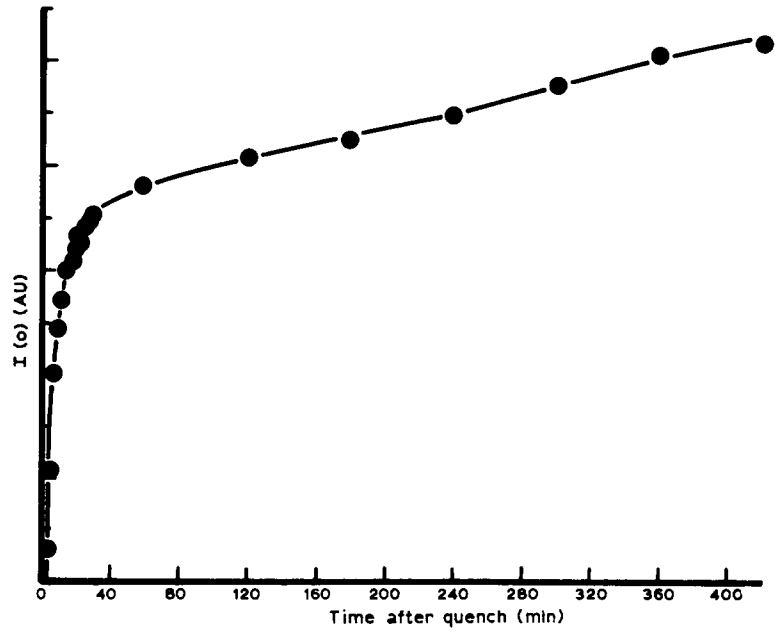


**Fig. 7.** Plot of $I(0)$ vs elapsed time after quenching. This plot shows the combination of results obtained using the synchrotron source ( < 30 min) and a conventional X-ray source ( > 30 min).

crystallization at longer times join smoothly with the changes in $I(0)$ measured at shorter times using the synchrotron source. Thus in the region where the modulus remains constant and $I(0)$ increases the changes in $I(0)$ can be attributed to crystallization. The turbidity of the formed gels, and the rapid development of turbidity during gelation (Miles *et al.*, 1984, 1985*b*), suggests that the spatial dimensions associated with the phase separation are compatible with optical wavelengths. The beam stop restricted the angular range probed in these synchrotron studies to $lql > 0{\cdot}02$ nm$^{-1}$. Thus the changes in the scattered intensity associated with the growth of these large domains will occur within the low $q$ region invisible behind the beam stop.

The only contributions to $I(0)$ obtained by extrapolating the experimental data will arise from local density changes occurring over spatial dimensions in the range of the X-ray measurements. Thus even the very early changes in $I(0)$ during development of the modulus probably monitor crystallization.

Since the rapid changes in modulus are concentration dependent, it is likely that amylose gelation proceeds by a phase separation into a polymer-rich network phase interpenetrated by a polymer-deficient

phase and is closely followed by crystallization, in extended-chain morphology, occurring in the rich phase independent of total polymer concentration. Since the shape of the crystalline regions changes little during the subsequent increase in crystallinity, it appears that nucleation is the dominant process.

## ACKNOWLEDGMENTS

This work was funded in part by the Ministry of Agriculture, Food and Fisheries.

## REFERENCES

Debye, P. & Bueche, A. M. (1949). *J. Appl. Phys.* **20,** 518.
Glatter, O. (1982). In *Small-Angle X-ray Scattering*, ed. O. Glatter and O. Kratky, Academic Press, London, p. 167.
Hashimoto, T., Kowsaka, K., Shibayama, M. & Suehiro, S. (1986). *Macromolecules* **19,** 750.
Khambatta, F. B., Warner, F., Russell, T. & Stein, R. S. (1976). *J. Polymer Sci., Polymer Phys. Ed.* **14,** 1391.
Miles, M. J., Morris, V. J. & Ring, S. G. (1984). *Carbohydr. Polym.* **4,** 93.
Miles, M. J., Morris, V. J., Orford, P. D. & Ring, S. G. (1985*a*). *Carbohydr. Res.* **135,** 271.
Miles, M. J., Morris, V. J.. & Ring, S. G. (1985*b*). *Carbohydr. Res.* **135,** 257.